

bonding rearrangement in two adjacent pyrroles. Thus, the two-electron oxidation leads from the tetraprotic porphyrinogen **1** to the diprotic ligand **6**. Four-electron oxidation should in principle lead to a nonprotic tetraaza macrocycle containing two such cyclopropane units.

Acknowledgment. We would like to thank the Fonds National Suisse de la Recherche Scientifique (Grant No. 20-28470-90) and Ciba-Geigy SA (Basel, Switzerland) for financial support. The Royal Society is also acknowledged for a European Science Fellowship to J.J.

Supplementary Material Available: Schakal drawings and complete listings of crystallographic data, fractional atomic coordinates, anisotropic thermal parameters, and bond distances and angles for complexes **4** and **5** (16 pages); listing of observed and calculated structure factors (61 pages). Ordering information is given on any current masthead page.

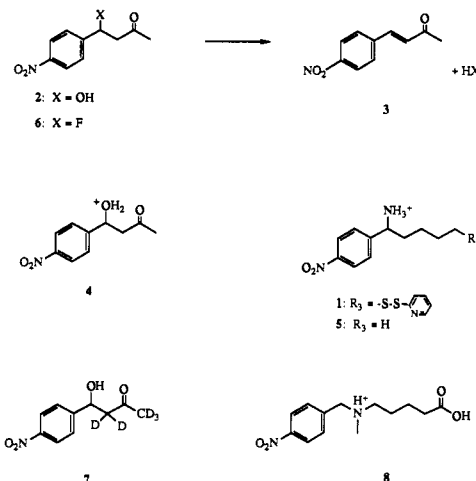


Figure 1. Haptens and substrates for the antibody-catalyzed dehydration reaction.

An Antibody-Catalyzed Dehydration Reaction

Tetsuo Uno[†] and Peter G. Schultz*

Department of Chemistry, University of California
Berkeley, California 94720

Received March 23, 1992

Enzymatic eliminations and additions of water, such as those involving dehydration of citrate, malate, and phosphoglycerate, represent an important class of biochemical reactions. One approach for generating antibodies that catalyze these reactions involves generating a combining site with a general base positioned for proton abstraction.¹ Alternatively, antibodies could be generated that stabilize the protonated form of the OH group, converting it to the much better leaving group, H₂O. In order to test this hypothesis, we asked whether antibodies generated against positively charged hapten **1** would catalyze the dehydration of β -hydroxy ketone **2** to enone **3** (Figure 1). Hapten **1** mimics the oxonium ion **4** formed by protonation of substrate by an active site amino acid residue or buffer.

Hapten **1** was synthesized by reduction of 4-benzoylbutyric acid to the corresponding keto alcohol with borane followed by reductive amination, nitration (cupric nitrate and trifluoroacetic anhydride),² and selective hydrolysis to afford 5-(nitrophenyl)-4-(trifluoroacetamido)pentanol. Formation of the tosylate followed by treatment with potassium thioacetate, deprotection with NaBH₄, and subsequent reaction with 2,2'-dithiobispyridine afforded hapten **1**.³ The hapten was conjugated to the thiolated carrier proteins, keyhole limpet hemocyanin (KLH) and bovine serum albumin, via a disulfide exchange reaction.⁴ Immunization with the KLH conjugate and generation of monoclonal antibodies were carried out as described previously.⁵ Antibodies were purified to homogeneity (as determined by SDS polyacrylamide gel electrophoresis and constant specific activity) by protein A affinity chromatography followed by cation exchange chromatography.⁶

The antibody-catalyzed dehydration of **2** to **3** was performed in 10 mM MES, MOPS, or CHES buffer of 100 mM ionic

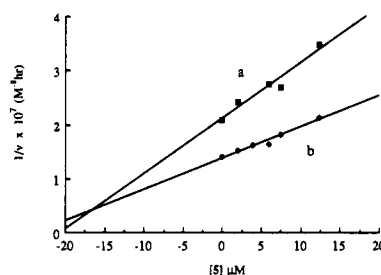


Figure 2. Competitive inhibition of antibody 20A2F6 by **5**. The concentration of 20A2F6 was 10 μ M in 10 mM MOPS, 95 mM NaCl, pH 7.0. Two concentrations of **2** were used: (a) 386 μ M; (b) 663 μ M.

strength adjusted with NaCl at 37 °C. The initial velocity was determined spectrophotometrically by monitoring the absorbance increase at 330 nm (products were confirmed by high-performance liquid chromatography).⁷ Antibody 20A2F6 showed the highest reaction rate acceleration compared to the uncatalyzed reaction. The reaction catalyzed by 20A2F6 demonstrates saturation kinetics: the kinetic constants K_m and k_{cat} were determined to be 1.1 mM and $2.1 \times 10^{-2} \text{ h}^{-1}$ (pH 7.0), respectively, by constructing a Hanes-Woolf plot.⁸ The pseudo-first-order rate constant of the background reaction in water (k'_{H_2O}) is $4.0 \times 10^{-5} \text{ h}^{-1}$, affording a value of $k_{cat}/k'_{H_2O} = 1200$.⁹ For comparison, the second-order rate constants of the acetic acid and acetate-catalyzed reactions (37 °C, 100 mM ionic strength) are $3 \times 10^{-4} \text{ M}^{-1} \text{ h}^{-1}$ and $0.7 \times 10^{-4} \text{ M}^{-1} \text{ h}^{-1}$, respectively.¹⁰ The catalytic activity of antibody 20A2F6 was competitively inhibited by the addition of the inhibitor **5** ($K_i = 16 \mu\text{M}$), demonstrating that catalysis takes place in the antibody combining site (Figure 2). In addition, antibody 20A2F6 does not catalyze the dehydration reaction of the isomeric *o*-nitrophenyl substrate to any detectable extent.¹¹

(7) The reaction was initiated by adding 20 μ L of a stock solution of the substrate in CH₃CN to 980 μ L of 10 μ M 20A2F6 in assay solution: $\Delta\epsilon_{280} = 16800$ was used to calculate the reaction rate. The concentration of 20A2F6 was determined by absorbance at 280 nm ($\epsilon(1 \text{ cm}; 0.1\%) = 1.37$) and 150000 for the molecular weight of IgG.

(8) Segel, I. H. *Enzyme Kinetics*; John Wiley and Sons: New York, 1975, p 210.

(9) The pseudo-first-order rate constant of the background reaction in water (k_{H_2O}) was determined by measuring velocities in the pH range between 5.5 and 6.5 (10 mM MES, 100 mM ionic strength adjusted with NaCl, 2% CH₃CN) at 37 °C. The background reaction rate was pH independent in this range, and the value of k_{H_2O} was calculated from the relation $v = k_{H_2O}[\text{H}_2\text{O}][\text{2}] = k'_{H_2O}[\text{2}]$.

(10) These values were determined by the method of Bell and Baugham: Bell, R. P.; Baugham, E. C. *J. Am. Chem. Soc.* **1937**, *59*, 4059.

(11) The β -hydroxy ketone substrates were synthesized by cross aldol condensation of acetone and 4'-nitrobenzaldehyde or 2'-nitrobenzaldehyde in the presence of a catalytic amount of sodium hydroxide and purified by silica gel chromatography (EtOAc/hexanes).

* Author to whom correspondence should be addressed.

[†] On leave from Kao Corp., Japan.

(1) (a) Shokat, K. M.; Leumann, C. J.; Sugawara, R.; Schultz, P. G. *Nature (London)* **1989**, *338*, 269-71. (b) Shokat, K. M.; Schultz, P. G. *Catalytic Antibodies*; John Wiley and Sons: 1991, pp 118-134.

(2) Crivello, J. J. *Org. Chem.* **1981**, *46*, 3056.

(3) Hapten **1** was purified by silica gel chromatography (EtOAc/EtOH) and characterized by NMR, mass spectrometry, infrared, and ultraviolet spectroscopy.

(4) Duncan, R. J. S., et al. *Anal. Biochem.* **1983**, *132*, 68-73.

(5) Jacobs, J.; Schultz, P. G.; Sugawara, R.; Powell, M. *J. Am. Chem. Soc.* **1987**, *109*, 2174-76.

(6) Kronvall, G.; Grey, H.; Williams, R. *J. Immunol.* **1970**, *105*, 1116.

The k_{cat} and K_m values for the deuterated substrate **7** are $6.5 \times 10^{-3} \text{ h}^{-1}$ and 0.90 mM , respectively, resulting in an isotope effect ($k_{\text{catH}}/k_{\text{catD}}$) of 3.3.¹² This suggests that the rate-determining transition state for the reaction involves some degree of α C-H bond breaking. For comparison, $(k_{\text{AcOH}})_{\text{H}}/(k_{\text{AcOH}})_{\text{D}} = 1.8$. Treatment of antibody with diazoacetamide had no effect on catalytic activity, suggesting either that glutamate or aspartate residues do not play a key catalytic role or that they are sequestered from the reagent.¹³ In contrast, treatment of antibody with 4'-nitro-2-bromoacetophenone led to complete inactivation, consistent with the presence of histidine, cysteine, serine, or lysine in the active site.¹⁴ Interestingly, antibody 43D4, which was generated to hapten **8** and catalyzes the elimination of HF from substrate **6**,¹ does not accelerate the dehydration of water from **2** (although it binds **2** with $K_D = 4.7 \text{ mM}$). This result is consistent with the notion that hapten **1** stabilizes an oxonium ion like transition state. Further experiments are being carried out to more precisely define the mechanism and stereochemistry of this antibody-catalyzed dehydration reaction and to generate an antibody combining site containing a catalytic dyad.

Acknowledgment. The authors acknowledge the Office of Naval Research (Grant No. N00014-91-J-1130) and Kao Corporation (T.U.) for support of this work. P.G.S. is a William M. Keck Foundation Investigator.

Registry No. **1**, 57548-40-0; **2**, 142160-94-9; **D**₂, 7782-39-0; dehydratase, 9044-86-4.

(12) The deuterated substrate **7** was synthesized from 4'-nitrobenzaldehyde and acetone-*d*₆.¹¹

(13) 20A2F6 was dialyzed against 20 mM borate and 150 mM NaClO₄ buffer, incubated with 0.4 M diazoacetamide at pH 5.5 at 25 °C for 8 h, and then dialyzed exhaustively against assay buffer. Grosberg, A. L.; Pressman, D. *J. Am. Chem. Soc.* **1960**, *82*, 5478-82.

(14) 20A2F6 was treated with 2 mM 4'-nitro-2-bromoacetophenone at room temperature for 50 h, pH 7, and dialyzed exhaustively against assay buffer. The control experiment with 4'-nitroacetophenone was carried out in a similar manner, and 20A2F6 showed no loss of catalytic activity.

Electron-Density Analysis of the Transition States of Substitution Reactions of 17- and 18-Electron Hexacarbonyl Complexes

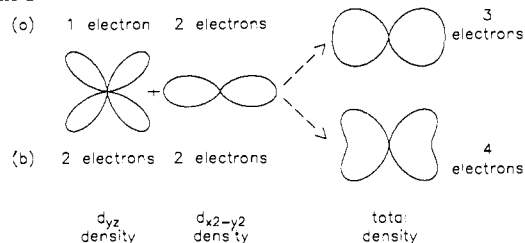
Zhenyang Lin and Michael B. Hall*

Department of Chemistry, Texas A&M University
College Station, Texas 77843

Received April 3, 1992

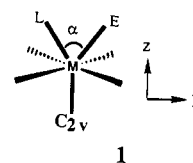
It is well known that 17-electron metal carbonyl radicals such as Mn(CO)₅ and Re(CO)₅ are substitution labile.¹⁻³ Kinetic studies have shown that the first CO substitution of the vanadium hexacarbonyl, V(CO)₆, by phosphine ligands is about 10¹⁰ times faster than that of the analogous 18-electron chromium complex, Cr(CO)₆.⁴ Usually, the substitutional lability of 17-electron metal complexes has been explained qualitatively in terms of formation of a 2-center, 3-electron bond in the 19-electron transition state or intermediate. However, the extremely large magnitude of the

Scheme I



rate enhancement is not yet satisfactorily understood through this simple bonding picture. In this communication, we provide an electron-density analysis of the 19-electron and 20-electron transition states and observe how the single electron difference leads to a significant difference in the valence-electron charge concentrations.

Restricted Hartree-Fock (RHF) ab initio calculations were used to obtain the electron density. The effective core potentials (ECPs) and double- ζ basis sets of Hay and Wadt were employed for transition-metal atoms.⁵ For ligand atoms, the ECPs and basis sets with a double- ζ representation of Stevens, Basch, and Krauss were used.⁶ Although we have shown that the electron correlation is extremely important for determining the transition states and activation energies of the substitution reactions of 17-electron and 18-electron carbonyl complexes, it is much less important for metals in the third transition series than in the first or second transition series.⁷ Therefore, for theoretical simplicity, we studied the transition states for carbonyl exchange reactions of $\text{M}(\text{CO})_6 + \text{CO}$ ($\text{M} = \text{Ta}$ and W) at the RHF level. The transition state (or intermediate if one exists) for an exchanging reaction can be easily obtained by optimizing structures with a symmetry (mirror or C_2) restriction relating the entering and leaving ligands, since the principle of microscopic reversibility requires that in the transition state (or intermediate) of an exchange reaction the entering and leaving groups have a like geometric relation to the rest of the structure.^{8,9} For nucleophilic attack on an octahedral face, the assumed transition state with a C_{2v} symmetry is shown in **1**. In the geometry optimization of the C_{2v} transition states, all degrees of freedom were optimized, except the M-C-O angles which were assumed to be linear for the four equivalent carbonyls.



For these assumed transition states, $\text{M}(\text{CO})_7$ (**1**), the structural parameters α and $\text{M}-\text{E}$ ($= \text{M}-\text{L}$, $\text{E} = \text{L} = \text{CO}$) are found to be 70.0° and 2.3 \AA for $\text{M} = \text{Ta}$ and 54.7° and 3.9 \AA for $\text{M} = \text{W}$. The assumed associative transition state for $\text{W}(\text{CO})_6 + \text{CO}$, in fact, resembles an I_d transition state since both entering and leaving ligands are far from the metal center in the calculated transition-state geometry. The activation energies are calculated to be 20.8 kcal/mol for the $\text{Ta}(\text{CO})_6 + \text{CO}$ exchange reaction and 35.8 kcal/mol for the $\text{W}(\text{CO})_6 + \text{CO}$ exchange reaction (the latter is close to the reported dissociation energy¹⁰). The significant activation energy difference (15.0 kcal/mol) can account for the extremely large magnitude of the rate enhancement, since the 10^{10} multiplicative difference in the substitution reaction rates corresponds to a difference of 12-13 kcal/mol in the activation energy if we assume an Arrhenius expression for the rate constant

(1) Kidd, D. R.; Brown, T. L. *J. Am. Chem. Soc.* **1978**, *100*, 4095.
(2) (a) Baird, M. C. *Chem. Rev.* **1988**, *88*, 1217. (b) Trogler, W. C. *Int. J. Chem. Kinet.* **1987**, *19*, 1025. (c) Howell, J. A. S.; Burkinshaw, P. M. *Chem. Rev.* **1983**, *83*, 557.

(3) (a) Basolo, F. *Inorg. Chim. Acta* **1985**, *100*, 3. (b) Basolo, F. *Polyhedron* **1990**, *9*, 1503. (c) Basolo, F. *Pure Appl. Chem.* **1988**, *60*, 1193. (d) Herrington, T. R.; Brown, T. L. *J. Am. Chem. Soc.* **1985**, *107*, 5700.

(4) (a) Shi, Q. Z.; Richmond, T. G.; Trogler, W. C.; Basolo, F. *J. Am. Chem. Soc.* **1982**, *102*, 4032. (b) Shi, Q. Z.; Richmond, T. G.; Trogler, W. C.; Basolo, F. *J. Am. Chem. Soc.* **1984**, *104*, 71. (c) Therien, M. J.; Trogler, W. C. *J. Am. Chem. Soc.* **1988**, *110*, 4942.

(5) Hay, P. J.; Wadt, W. R. *J. Chem. Phys.* **1985**, *82*, 299.

(6) Stevens, W. J.; Basch, H.; Krauss, M. *J. Chem. Phys.* **1984**, *81*, 6026.

(7) Lin, Z.; Hall, M. B. *Inorg. Chem.*, in press.

(8) Lin, Z.; Hall, M. B. *Inorg. Chem.* **1991**, *30*, 646.

(9) Frost, A. A.; Pearson, R. G. *Kinetics and Mechanism*; John Wiley: New York, 1953.

(10) Lewis, K. E.; Golden, D. M.; Smith, G. P. *J. Am. Chem. Soc.* **1984**, *106*, 3906.